First-principles-based Landau-Devonshire potential for $BiFeO_3$

P. Marton,[1,2,*] A. Klíč,[1] M. Paściak,[1] and J. Hlinka[1]

[1]*Institute of Physics, Academy of Sciences of the Czech Republic Na Slovance 2, 182 21 Prague 8, Czech Republic*

[2]*Institute of Mechatronics and Computer Engineering, Technical University of Liberec Studentská 2, 461 17 Liberec, Czech Republic*

(Received 6 June 2017; published 17 November 2017)

The work describes a first-principles-based computational strategy for studying structural phase transitions, and in particular, for determination of the so-called Landau-Devonshire potential—the classical zero-temperature limit of the Gibbs energy, expanded in terms of order parameters. It exploits the configuration space attached to the eigenvectors of the modes frozen in the ground state, rather than the space spanned by the unstable modes of the high-symmetry phase, as done usually. This allows us to carefully probe the part of the energy surface in the vicinity of the ground state, which is most relevant for the properties of the ordered phase. We apply this procedure to $BiFeO_3$ and perform *ab initio* calculations in order to determine potential energy contributions associated with strain, polarization, and oxygen octahedra tilt degrees of freedom, compatible with its two-formula unit cell periodic boundary conditions.

DOI: 10.1103/PhysRevB.96.174110

Phenomenological models, taking into account important structural order parameters and coupling between them, can greatly help to grasp the physical mechanisms involved in various crystal structure based phenomena, such as piezoelectricity, ferroelectricity, electrostriction, etc. Typically, when simple models for structural phase transitions are derived from first-principles calculations, the microscopic order parameters relevant for a structural phase transition are selected from unstable phonon modes of the high-symmetry reference phase. Then, the configurational space attached to the Landau-Devonshire (LD) potential (the zero temperature limit of the Gibbs free energy functional) is defined by perturbation of the high-symmetry state along the coordinates associated with these unstable modes [1–5].

Here we present an alternative approach consisting of the adjustment of the LD potential landscape in the vicinity of the ground state configuration, which is the most relevant region of the order parameter space when the ordered phase itself is the focus of interest. This is particularly important when the high-temperature phase and the ordered ground state have rather distinct atomic and electronic structures. It actually happens for many materials showing phase transitions at high temperatures.

An interesting material, where such an approach is desirable, is the ferroelectric $BiFeO_3$—an insulating material with a metallic paraelectric phase, known by its large spontaneous polarization and a high T_C [6–8]. The symmetry-breaking order parameters of its ferroelectric $Pm\bar{3}m > R3c$ phase transition, namely the ferroelectric polarization vector **P** and the oxygen-octahedron tilt vector **A**, are in our approach associated with the atomic displacement patterns frozen in the fully relaxed ground state. Therefore, the eigenvectors of the high-symmetry phase dynamical matrix are not used here. Actually, in this particular case, the atomic-displacement patterns associated with the **P** and **A** vectors together with the spontaneous deformation tensor **e** define the difference between the reference and the ground state completely.

The energy profiles along selected paths connecting the reference paraelectric state with ($\mathbf{P}=0$, $\mathbf{A}=0$, and $\mathbf{e}=0$) to the *ab initio* ground state ($\mathbf{P}=\mathbf{P}_s$, $\mathbf{A}=\mathbf{A}_s$, and $\mathbf{e}=\mathbf{e}_s$), defined in Table I, are shown in Fig. 1. We believe that the numerical values of the LD potential parameters given in this work can be readily used for a variety of purposes such as an estimation of nonlinear electromechanical properties of $BiFeO_3$, evaluation of the influence of the epitaxial strain, or in a range of phase-field modeling tasks.

Analytic form of the potential. The LD potential (zero-temperature potential density) f considered here is expanded around the reference paraelectric state in the usual form of the symmetry-restricted Taylor expansion in terms of 12 independent variables, covering the selected set of order parameters $\mathbf{P}=(P_x,P_y,P_z)$, $\mathbf{A}=(A_x,A_y,A_z)$, and $\mathbf{e}=(e_{xx},e_{yy},e_{zz},e_{yz},e_{xz},e_{xy})$. The resulting form can be expressed as a sum

$$f = f_a^{(e)}[\{P_i\}] + f_b^{(e)}[\{A_i\}] + f_t^{(e)}[\{P_i,A_i\}] + f_{est}[\{P_i,e_{ij}\}] + f_{rst}[\{A_i,e_{ij}\}] + f_{ela}[\{e_{ij}\}]. \quad (1)$$

The first three contributions describe the energy expansion in terms of the ferroelectric polarization and the oxygen octahedron tilt only. They have been expanded till eighth order because stopping at the sixth order did not reproduce the *ab initio* calculated potential landscape satisfactorily. The ferroelectric part of the Landau energy $f_a^{(e)}$ contains all symmetry-allowed terms

$$f_a^{(e)} = a_i P_i^2 + a_{ij}^{(e)} P_i^2 P_j^2 + a_{ijk} P_i^2 P_j^2 P_k^2 + a_{ijkl} P_i^2 P_j^2 P_k^2 P_l^2, \quad (2)$$

and the same holds for the $f_b^{(e)}$, which has the same form but in terms of angles $\{A_i\}$ and coefficients b. The coupling between polarization and oxygen octahedron tilt is described by

$$\begin{aligned} f_t^{(e)} = {} & t_{ijkl}^{(e)} P_i P_j A_k A_l + t_{ijklmn}^{42} P_i P_j P_k P_l A_m A_n \\ & + t_{ijklmn}^{24} P_i P_j A_k A_l A_m A_n \\ & + t_{ijklmnpq}^{44} P_i P_j P_k P_l A_m A_n A_p A_q \\ & + t_{ijklmnpq}^{62} P_i P_j P_k P_l P_m P_n A_p A_q \\ & + t_{ijklmnpq}^{26} P_i P_j A_k A_l A_m A_n A_p A_q, \end{aligned} \quad (3)$$

*marton@fzu.cz

TABLE I. Paths in the order-parameter space, sampled by a path parameter ξ, for which the first-principles energies were evaluated and plotted in Fig. 1. The last column corresponds to the position of the calculated point on the horizontal axis in Fig. 1.

	$P_i/(P_s)_i$	$A_i/(A_s)_i$	$e_{ij}/(e_s)_{ij}$	x
1	(ξ,ξ,ξ,	0,0,0,	0,0,0,0,0,0)	ξ
2	(0,0,0,	ξ,ξ,ξ,	0,0,0,0,0,0)	ξ
3	(0,0,0,	0,0,0,	ξ,ξ,ξ,ξ,ξ,ξ)	ξ
4	(1,1,1,	ξ,ξ,ξ,	0,0,0,0,0,0)	$1+\xi$
5	(1,1,1,	0,0,0,	ξ,ξ,ξ,ξ,ξ,ξ)	$1+\xi$
6	(ξ,ξ,ξ,	1,1,1,	0,0,0,0,0,0)	$1+\xi$
7	(0,0,0,	1,1,1,	ξ,ξ,ξ,ξ,ξ,ξ)	$1+\xi$
8	(ξ,ξ,ξ,	0,0,0,	1,1,1,1,1,1)	$1+\xi$
9	(0,0,0,	ξ,ξ,ξ,	1,1,1,1,1,1)	$1+\xi$
10	(ξ,ξ,ξ,	1,1,1,	1,1,1,1,1,1)	$2+\xi$
11	(1,1,1,	ξ,ξ,ξ,	1,1,1,1,1,1)	$2+\xi$
12	(1,1,1,	1,1,1,	ξ,ξ,ξ,ξ,ξ,ξ)	$2+\xi$
13	(ξ,ξ,ξ,	ξ,ξ,ξ,	ξ,ξ,ξ,ξ,ξ,ξ)	3ξ

we have included all symmetry allowed terms up to the sixth order, while the eighth order terms were limited to the pair interaction between single P_i and single A_i components only. On the other hand, since the strain contribution to the ground state LD energy is rather small, only the lowest-order coupling and self-energy terms in strain were introduced. Their role is to describe electrostriction, rotostriction (introduced in an obvious analogy to electrostriction), and elastic energy contributions, respectively:

$$f_{\rm est} = -q_{ijkl}e_{ij}P_kP_l, \quad f_{\rm rot} = -r_{ijkl}e_{ij}A_kA_l,$$
$$f_{\rm ela} = \tfrac{1}{2}C_{ijkl}e_{ij}e_{kl}. \qquad (4)$$

Let us note that the term including all three order parameters is not included and that the adopted potential form allows a straightforward analytical elimination of the strain degree

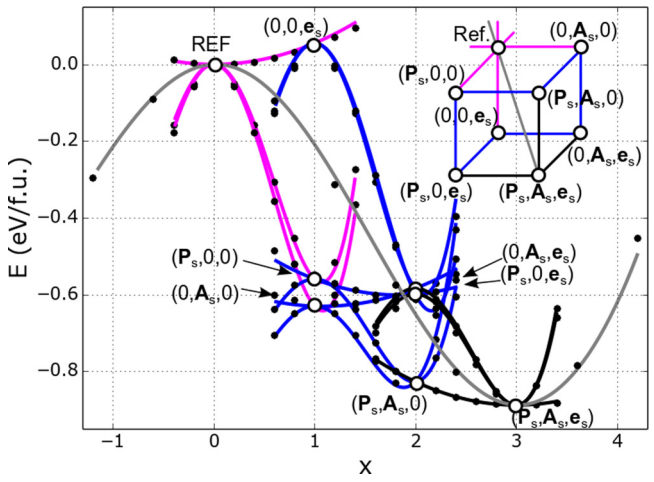

FIG. 1. Energy profiles along selected paths in the order-parameter space of $BiFeO_3$, connecting the cubic reference state (REF) and the ground state ($\mathbf{P}_s$,$\mathbf{A}_s$,$\mathbf{e}_s$). Point symbols stand for direct first-principles calculations, lines are evaluated from the present LD potential. Individual path segments are depicted in the inset and described in detail in Table I.

of freedom using linear equations of mechanical equilibrium [9,10], which facilitates considerations about a mechanically free crystal.

The superscript (e) marks the terms and parameters which are renormalized upon such strain elimination, and it emphasizes that they are related to a material clamped to the reference cubic shape.

First-principles-calculations details. The total-energy calculations are based on density functional theory (DFT) within the local spin-density approximation with Hubbard U-correction (LSDA+U), as implemented in the Vienna *ab initio* simulation package (VASP) [11,12]. The projector-augmented plane-wave method was used [13]. There were 15 explicitly treated electrons for Bi ($5d^{10}$ $6s^2$ $6p^3$), 14 for Fe ($3p^6$ $4s^1$ $3d^7$), and 6 for oxygen ($2s^2$ $2p^4$). The energy cutoff for plane waves was set to 500 eV. The Brillouin-zone integrations were carried out using 3×3×3 Monkhorst-Pack k-point mesh [14]. Gaussian broadening of 0.1 eV was applied [15]. The antiferromagnetic (AFM) G-type order on Fe atoms has been taken into account. The LSDA+U method is applied in all calculations, with the Hubbard term [16] added to the iron d orbitals. In the used Dudarev [17] approach the difference U-J was set to 3.0 eV in order to reproduce the structural properties of $BiFeO_3$.

All calculations presented here were performed using a 10-atom rhombohedral supercell of $BiFeO_3$ compatible with the G-type AFM order. The two perovskite cells in the supercell host two oppositely rotated oxygen octahedra. The tilt vector **A** discussed in the text always refers to the axial rotation vector of the oxygen octahedron in the first cell, while the rotation in the other cell is automatically opposite ($-\mathbf{A}$). Polarization vector **P** is the same in both perovskite cells.

Microscopic representation of the selected order parameters. As a starting point in the presented procedure the atomic structures of the reference cubic state and the rhombohedral ground state of the $BiFeO_3$ were determined. These are fully optimized using first-principles calculations within the cubic and $R3c$ symmetries, respectively. The cubic unit cell is characterized by $a = 5.438$ Å and $\alpha = 60^\circ$, while the $R3c$ ground state is described by the cell with $a = 5.517$ Å and $\alpha = 59.866^\circ$ and fractional atomic coordinates $\mathrm{Bi}(2a)_x = 0$, $\mathrm{Fe}(2a)_x = 0.227$, and $\mathrm{O}(6b) = (0.541,\ 0.942,\ 0.395)$, in a good agreement with the available theoretical [8,18] and experimental [19] data.

The difference between the ground state and the reference configurations can be specified by differences in fractional atomic coordinates $\Delta\mathbf{u}_s$ and by the change of the supercell lattice vectors. Evaluation of the strain tensor is a straightforward procedure, because the lattice vectors of any slightly distorted unit cell described by the tensor of deformation **e** can be obtained by applying the $\mathbf{1}+\mathbf{e}$ matrix multiplication operation to the three reference-state lattice vectors. However, the $\Delta\mathbf{u}_s$ (which is a 30-component vector for the ten-atom $BiFeO_3$ supercell) requires more attention. It can be further decomposed into two parts, $\Delta\mathbf{u}_s^{(a)} + \Delta\mathbf{u}_s^{(b)}$. The first part, which transforms as the (111) component of the F_{1u} Brillouin-zone-center polar mode of the parent cubic phase, defines displacements $\Delta\mathbf{u}_s^{(a)}$ related to the spontaneous ferroelectric polarization $\mathbf{P}_s \parallel (111)$, while the remaining part $\Delta\mathbf{u}_s^{(b)}$, transforming as the Brillouin-zone-corner irreducible

representation, defines the spontaneous oxygen octahedron tilt $\mathbf{A}_s \parallel (111)$. This decomposition is thus unique.

Furthermore, we have assumed that the space of vectors **P** are attached to a single zone-center mode, i.e., to a mode with a fixed atomic pattern. In other words, the atomic displacements corresponding to the polarization $\mathbf{P} = \xi \mathbf{P}_s$ are given by $\Delta\mathbf{u}^{(a)} = \xi \Delta\mathbf{u}_s^{(a)}$ and the atomic displacements corresponding to the polarization **P** equal to the spontaneous one but directed along, say (100) Cartesian direction, are obtained by rotation of each individual atomic displacement vector comprised in $\Delta\mathbf{u}_s^{(a)}$ by the same proper rotation that turns (111) into (100) direction in the space of the attached polarization vectors **P**. Similar procedure is applied to relate $\Delta\mathbf{u}_s^{(b)}$ with **A**. This construction defines a consistent linear subspace of the atomic coordinates, compatible with the $Z = 2$ supercell boundary conditions.

Fitting parameters of the Landau-Devonshire potential. The described procedure establishes a one-to-one correspondence between a point in the order-parameter space and the atomic structure. Using this link, it is possible to sample the parameter space, to use first-principles calculations to determine energies, and to fit the energy surface in order to obtain parameters of the potential.

The individual terms in (1) are fitted separately. For each term, a suitable set of paths was chosen. For example, to fit the parameters a's in the $f_a^{(e)}(\{P_i\})$, several paths along the high symmetry directions in the polarization space were chosen, while keeping the oxygen octahedra tilt and strain zero. Angular dependence of energy on polarization vector was probed employing circular paths around the paraelectric reference state with several different diameters and orientations of the circles. Similar procedure was then adopted for $f_b^{(e)}(\{A_i\})$. In evaluation of the coupling terms, e.g., between polarization and tilt, we subtract the already determined contribution of polarization and tilt and fit only the energy difference corresponding to the coupling energy. The so obtained set of parameters is consequently utilized as an initial condition for fitting of all parameters together under an additional constraint ensuring that the position of the global minimum of the potential corresponds exactly to the ground state obtained from first principles. This fitting procedure has been conveniently accomplished in dimensionless variables normalized to the ground state values of $\Delta\mathbf{u}_s^{(a)}$, $\Delta\mathbf{u}_s^{(b)}$, and $\mathbf{e}_s$. The final set of the numerical values defining the LD potential parameters of $BiFeO_3$ were rescaled with spontaneous values $(\mathbf{e}_s)_{xx} = 0.136$, $(\mathbf{e}_s)_{xy} = 0.0012$, $A_s = |\mathbf{A}_s| = 14.355$ deg (our *ab initio* data), and $P_s = |\mathbf{P}_s| = 0.91\,\mathrm{C/m^2}$ (adopted from Ref. [20]). Resulting Landau-Devonshire model for $BiFeO_3$ is given in Table II.

The energy profiles of the LD potential along several important directions in the order-parameter space (paths listed in Table I) are displayed in Fig. 1. The direct *ab initio*-calculated energies, presented as dots in the figure, exhibit visually perfect agreement with the predictions of the fitted LD potential. Therefore, it can be expected that the present potential also describes well the various linear response properties, in particular within its ground state. For example, the elastic tensor of $BiFeO_3$ predicted by second-order strain derivatives of the present LD potential in its rhombohedral ground state compares fairly well with other literature data (see

TABLE II. Coefficients of the LD potential for $BiFeO_3$. The second column provides one representant of symmetry-equivalent terms associated with the respective coefficient, and the third column gives the numerical value of the coefficient or its simple multiple, indicated in the first column.

	Type	SI	Unit
a_1	P_x^2	-3.362×10^9	$\mathrm{J\,m\,C^{-2}}$
$a_{11}^{(e)}$	P_x^4	2.646×10^9	$\mathrm{J\,m^5\,C^{-4}}$
$2a_{12}^{(e)}$	$P_x^2 P_y^2$	3.274×10^9	$\mathrm{J\,m^5\,C^{-4}}$
a_{111}	P_x^6	-5.960×10^8	$\mathrm{J\,m^9\,C^{-6}}$
$3a_{112}$	$P_x^4 P_y^2$	2.634×10^8	$\mathrm{J\,m^9\,C^{-6}}$
$6a_{123}$	$P_x^2 P_y^2 P_z^2$	-7.132×10^9	$\mathrm{J\,m^9\,C^{-6}}$
a_{1111}	P_x^8	9.043×10^7	$\mathrm{J\,m^{13}\,C^{-8}}$
$4a_{1112}$	$P_x^6 P_y^2$	-2.284×10^8	$\mathrm{J\,m^{13}\,C^{-8}}$
$6a_{1122}$	$P_x^4 P_y^4$	4.636×10^8	$\mathrm{J\,m^{13}\,C^{-8}}$
$12a_{1123}$	$P_x^4 P_y^2 P_z^2$	1.493×10^9	$\mathrm{J\,m^{13}\,C^{-8}}$
b_1	A_x^2	-1.585×10^7	$\mathrm{J\,m^{-3}\,deg^{-2}}$
$b_{11}^{(e)}$	A_x^4	5.396×10^4	$\mathrm{J\,m^{-3}\,deg^{-4}}$
$2b_{12}^{(e)}$	$A_x^2 A_y^2$	6.314×10^4	$\mathrm{J\,m^{-3}\,deg^{-4}}$
b_{111}	A_x^6	-6.598×10^1	$\mathrm{J\,m^{-3}\,deg^{-6}}$
$3b_{112}$	$A_x^4 A_y^2$	-5.203×10^1	$\mathrm{J\,m^{-3}\,deg^{-6}}$
$6b_{123}$	$A_x^2 A_y^2 A_z^2$	-5.910×10^1	$\mathrm{J\,m^{-3}\,deg^{-6}}$
b_{1111}	A_x^8	4.890×10^{-2}	$\mathrm{J\,m^{-3}\,deg^{-8}}$
$4b_{1112}$	$A_x^6 A_y^2$	1.598×10^{-2}	$\mathrm{J\,m^{-3}\,deg^{-8}}$
$6b_{1122}$	$A_x^4 A_y^4$	1.194×10^{-1}	$\mathrm{J\,m^{-3}\,deg^{-8}}$
$12b_{1123}$	$A_x^4 A_y^2 A_z^2$	1.002×10^{-1}	$\mathrm{J\,m^{-3}\,deg^{-8}}$
$t_{1111}^{(e)}$	$P_x^2 A_x^2$	1.720×10^7	$\mathrm{J\,m\,C^{-2}\,deg^{-2}}$
$t_{1122}^{(e)}$	$P_x^2 A_y^2$	2.273×10^7	$\mathrm{J\,m\,C^{-2}\,deg^{-2}}$
$4t_{1212}^{(e)}$	$P_x P_y A_x A_y$	-2.844×10^7	$\mathrm{J\,m\,C^{-2}\,deg^{-2}}$
t_{111111}^{42}	$P_x^4 A_x^2$	2.371×10^6	$\mathrm{J\,m^5\,C^{-4}\,deg^{-2}}$
t_{111111}^{24}	$P_x^2 A_x^4$	-5.689×10^4	$\mathrm{J\,m\,C^{-2}\,deg^{-4}}$
t_{111122}^{42}	$P_x^4 A_y^2$	-9.069×10^6	$\mathrm{J\,m^5\,C^{-4}\,deg^{-2}}$
t_{112222}^{24}	$P_x^2 A_y^4$	-4.608×10^4	$\mathrm{J\,m\,C^{-2}\,deg^{-4}}$
$6t_{112233}^{42}$	$P_x^2 P_y^2 A_z^2$	-8.438×10^6	$\mathrm{J\,m^5\,C^{-4}\,deg^{-2}}$
$6t_{112233}^{24}$	$P_x^2 A_y^2 A_z^2$	-2.421×10^4	$\mathrm{J\,m\,C^{-2}\,deg^{-4}}$
$6t_{112211}^{42}$	$P_x^2 P_y^2 A_x^2$	6.805×10^6	$\mathrm{J\,m^5\,C^{-4}\,deg^{-2}}$
$6t_{111122}^{24}$	$P_x^2 A_x^2 A_y^2$	2.594×10^4	$\mathrm{J\,m\,C^{-2}\,deg^{-4}}$
$8t_{111212}^{42}$	$P_x^3 P_y A_x A_y$	-1.954×10^7	$\mathrm{J\,m^5\,C^{-4}\,deg^{-2}}$
$24t_{123312}^{42}$	$P_x P_y P_z^2 A_x A_y$	2.660×10^7	$\mathrm{J\,m^5\,C^{-4}\,deg^{-2}}$
$8t_{121112}^{24}$	$P_x P_y A_x^3 A_y$	-8.314×10^3	$\mathrm{J\,m\,C^{-2}\,deg^{-4}}$
$24t_{121233}^{24}$	$P_x P_y A_x A_y A_z^2$	-5.457×10^4	$\mathrm{J\,m\,C^{-2}\,deg^{-4}}$
$t_{11111111}^{62}$	$P_x^6 A_x^2$	-2.573×10^6	$\mathrm{J\,m^9\,C^{-6}\,deg^{-2}}$
$t_{11111111}^{26}$	$P_x^2 A_x^6$	1.132×10^2	$\mathrm{J\,m\,C^{-2}\,deg^{-6}}$
$t_{11111122}^{62}$	$P_x^6 A_y^2$	1.370×10^6	$\mathrm{J\,m^9\,C^{-6}\,deg^{-2}}$
$t_{11222222}^{26}$	$P_x^2 A_y^6$	5.255×10^1	$\mathrm{J\,m\,C^{-2}\,deg^{-6}}$
$t_{11111111}^{44}$	$P_x^4 A_x^4$	4.747×10^4	$\mathrm{J\,m^5\,C^{-4}\,deg^{-4}}$
$t_{11112222}^{44}$	$P_x^4 A_y^4$	1.888×10^4	$\mathrm{J\,m^5\,C^{-4}\,deg^{-4}}$
q_{1111}	$e_{xx} P_x^2$	1.447×10^{10}	$\mathrm{J\,m\,C^{-2}}$
q_{1122}	$e_{xx} P_y^2$	4.776×10^9	$\mathrm{J\,m\,C^{-2}}$
$2q_{1212}$	$e_{xy} P_x P_y$	7.186×10^9	$\mathrm{J\,m\,C^{-2}}$
r_{1111}	$e_{xx} A_x^2$	2.319×10^7	$\mathrm{J\,m^{-3}\,deg^{-2}}$
r_{1122}	$e_{xx} A_y^2$	-4.886×10^6	$\mathrm{J\,m^{-3}\,deg^{-2}}$
$2r_{1212}$	$e_{xy} A_x A_y$	-2.526×10^7	$\mathrm{J\,m^{-3}\,deg^{-2}}$
C_{1111}	e_{xx}^2	2.666×10^{11}	Pa
C_{1122}	$e_{xx} e_{yy}$	1.435×10^{11}	Pa
C_{1212}	e_{xy}^2	9.548×10^{10}	Pa

TABLE III. Elastic stiffness constants of rhombohedral $BiFeO_3$ ground state (the sign of C_{14} depends on adopted coordinate system).

	C_{11}	C_{12}	C_{13}	C_{14}	C_{33}	C_{44}	C_{66}
LD potential (this work)	278	122	95	−22	228	57	78
LDA calculations (this work)	264	147	63	−16	132	53	54
Borissenko *et al.* [21], LDA	249	151	75	9	160	44	49
Shang *et al.* [22], GGA	222	110	50	16	150	49	56

Table III). As an even more representative performance test, we have generated 300 random configurations with the 12 order-parameter components falling within ±20 percent around their spontaneous values and calculated their total energies from the LD potential as well as from the first principles. The agreement is also satisfactory (see Fig. 2). Moreover, since the present potential goes well behind the so far adopted quartic anharmonicity in the polarization and tilt degrees of freedom [23–27], one can expect that the this LD potential will be more appropriate when dealing with nonlinear responses.

To conclude, we present a comprehensive and efficient procedure for extraction of the Landau-Devonshire-type potential from quantum-mechanical calculations. We believe that this scheme, based on the microscopic content of order parameters derived from the full-amplitude distortions of the low-symmetry phase ground state, will enable a real methodological progress for systematic development of models for a large family of materials with structural phase transitions. In the specific case of the prototypical multiferroic material $BiFeO_3$, we present a carefully engineered Landau-Devonshire potential, which can be readily used for analytical calculations or numerical simulations, for which realistic intrinsic properties are crucial. By accurate fitting and taking into account an extensive form of the potential, we have targeted to enhance the scope of its applicability to various

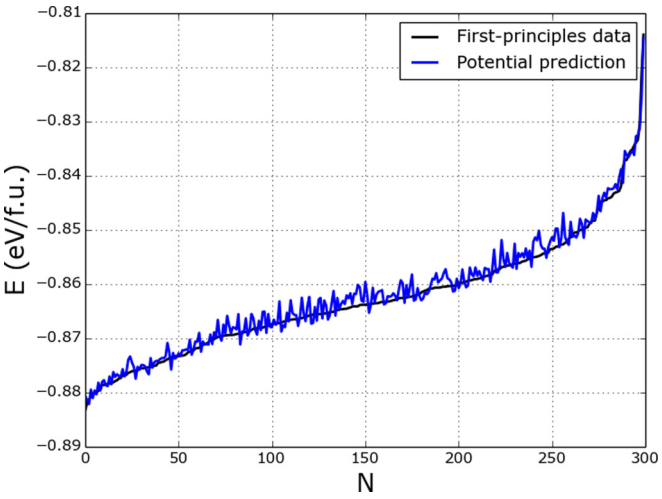

FIG. 2. Comparison of first-principles and LD-predicted energies for 300 randomly selected points in the order-parameters space in the vicinity of the rhombohedral ground state (coordinates falling within 20 percent around the ground state values). Monotonously increasing function stands for the direct first-principles data, ordered by the increasing total energy, while the fluctuating curve connects the corresponding energies, calculated from the LD potential.

metastable configurations. We believe that the potential and its applications will improve understanding of $BiFeO_3$, serve as a basis for further development, as well as open an avenue for computationally supported engineering of $BiFeO_3$-based functional structures, such as heterostructures or thin films.

Acknowledgments. This work was supported by the Czech Science Foundation (Project No. 15-04121S). Access to computing and storage facilities owned by parties and projects contributing to the National Grid Infrastructure MetaCentrum provided under the programme "Projects of Large Research, Development, and Innovations Infrastructures" (CESNET LM2015042), is greatly appreciated.

[1] W. Zhong, D. Vanderbilt, and K. M. Rabe, Phys. Rev. Lett. **73**, 1861 (1994).
[2] K. Rabe, C. H. Ahn, and J.-M. Triscone, *Physics of Ferroelectrics: A Modern Perspective* (Springer, Berlin, 2007).
[3] A. Paul, J. Sun, J. P. Perdew, and U. V. Waghmare, Phys. Rev. B **95**, 054111 (2017).
[4] S. M. Nakhmanson and I. Naumov, Phys. Rev. Lett. **104**, 097601 (2010).
[5] G. H. Olsen, U. Aschauer, N. A. Spaldin, S. M. Selbach, and T. Grande, Phys. Rev. B **93**, 180101(R) (2016).
[6] G. Catalan and J. F. Scott, Adv. Mater. **21**, 2463 (2009).
[7] D. Sando, A. Barthoélémy, and M. Bibes, J. Phys.: Condens. Matter **26**, 473201 (2014).
[8] J. B. Neaton, C. Ederer, U. V. Waghmare, N. A. Spaldin, and K. M. Rabe, Phys. Rev. B **71**, 014113 (2005).
[9] S. Nambu and D. A. Sagala, Phys. Rev. B **50**, 5838 (1994).
[10] J. Hlinka and P. Marton, Phys. Rev. B **74**, 104104 (2006).
[11] G. Kresse and J. Hafner, Phys. Rev. B **47**, 558 (1993).
[12] G. Kresse and J. Furthmüller, Phys. Rev. B **54**, 11169 (1996).
[13] P. E. Blöchl, Phys. Rev. B **50**, 17953 (1994).
[14] H. J. Monkhorst and J. D. Pack, Phys. Rev. B **13**, 5188 (1976).
[15] C. L. Fu and K. M. Ho, Phys. Rev. B **28**, 5480 (1983).
[16] V. I. Anisimov, F. Aryasetiawan, and A. I. Lichtenstein, J. Phys.: Condens. Matter **9**, 767 (1997).
[17] S. L. Dudarev, G. A. Botton, S. Y. Savrasov, C. J. Humphreys, and A. P. Sutton, Phys. Rev. B **57**, 1505 (1998).
[18] M. Graf, M. Sepliarsky, M. Stachiotti, and S. Tinte, Ferroelectrics **461**, 61 (2014).
[19] D. C. Arnold, K. S. Knight, F. D. Morrison, and P. Lightfoot, Phys. Rev. Lett. **102**, 027602 (2009).
[20] O. Diéguez, O. E. González-Vázquez, J. C. Wojdeł, and J. Íñiguez, Phys. Rev. B **83**, 094105 (2011).
[21] E. Borissenko, M. Goffinet, A. Bosak, P. Rovillain, M. Cazayous, D. Colson, P. Ghosez, and M. Krisch, J. Phys.: Condens. Matter **25**, 102201 (2013).

[22] S. L. Shang, G. Sheng, Y. Wang, L. Q. Chen, and Z. K. Liu, Phys. Rev. B **80**, 052102 (2009).
[23] F. Xue, Y. Gu, L. Liang, Y. Wang, and L.-Q. Chen, Phys. Rev. B **90**, 220101(R) (2014).
[24] M. Daraktchiev, G. Catalan, and J. F. Scott, Phys. Rev. B **81**, 224118 (2010).
[25] N. E. Kulagin, A. F. Popkov, S. V. Solovev, K. S. Sukmanova, and A. K. Zvezdin, Phys. Solid State **57**, 933 (2015).
[26] I. A. Kornev, S. Lisenkov, R. Haumont, B. Dkhil, and L. Bellaiche, Phys. Rev. Lett. **99**, 227602 (2007).
[27] I. A. Kornev, L. Bellaiche, P.-E. Janolin, B. Dkhil, and E. Suard, Phys. Rev. Lett. **97**, 157601 (2006).